

Fluoride-Induced Neuron Apoptosis and Expressions of Inflammatory Factors by Activating Microglia in Rat Brain

Nan Yan^{1,2} · Yan Liu² · Shengnan Liu¹ · Siqi Cao¹ · Fei Wang¹ · Zhengdong Wang² · Shuhua Xi¹

Received: 26 April 2015 / Accepted: 27 July 2015 / Published online: 8 August 2015
© Springer Science+Business Media New York 2015

Abstract Excessive exposure to fluoride results in structural and functional damages to the central nervous system (CNS), and neurotoxicity of fluoride may be associated with neurodegenerative changes. Chronic microglial activation appears to cause neuronal damage through producing proinflammatory cytokines and is involved in many neurodegenerative disorders. It is not known about effects on microglia of fluoride. In the present study, healthy adult Wistar rats were exposed to 60 and 120 ppm fluoride in drinking water for 10 weeks, and control rats received deionized water. After 10 weeks, rats were sacrificed under anesthesia then apoptosis in neuron and inflammatory factors secreted by microglia were determined. We found that apoptosis of neurons in fluoride-treated rat brain increased and terminal deoxynucleotidyl transferase-mediated dUTP nick-end labeling (TUNEL)-positive immunofluorescence increased with increasing fluoride concentrations. Bax protein expression increased and Bcl-2 protein expression decreased in fluoride-treated rat brain compared with that of the control rat brain. The microglia in the hippocampus and cortex of fluoride-treated rats were activated by immunostaining with OX-42, a marker of activated

microglia, and OX-42-positive microglia cells were more abundant in the hippocampus than in the cortex. The levels of IL-1 β and IL-6 protein expression in OX-42-labeled microglial cells were significantly increased in the cortex and hippocampus of rats exposed to fluoride, and TNF- α immunoreactivity in microglial cells of the hippocampus was significantly higher in the 120 ppm fluoride-treated group than that in the control group. Our results indicate that fluoride induced neuron apoptosis and expressions of inflammatory factors by activating microglia in rat brain.

Keywords Fluoride · Microglia · Inflammatory factors · Apoptosis · Rat brain

Introduction

Excessive fluoride may cross the blood–brain barrier and accumulate in the brain, causing dysfunction of the central nervous system (CNS). Epidemiological investigations have revealed that the intelligence quotient (IQ) of children living in high fluoride areas was lower than that of children living in low fluoride areas [1–3]. A meta-analysis showed that children who live in a fluorosis area have five times higher odds of developing low IQ than those who live in a nonfluorosis area or a slight fluorosis area [4]. Psychiatric symptoms such as lethargy, memory and concentration impairment, and thinking difficulties appeared after chronic exposure to industrial fluoride in workers [5]. In the animal experiments, fluoride decreased the number of avoidance responses in the active avoidance task in rats and had potentially deleterious effects on learning and memory [6]. The learning abilities and memory of high-fluoride exposure mice were significantly lower than those of the control group [7]. The neuropathological

✉ Shuhua Xi
shxi@mail.cmu.edu.cn

¹ Department of Occupational and Environmental Health, School of Public Health, China Medical University, No. 77 Puhe Road, Shenyang North New Area, Shenyang, Liaoning Province 110122, People's Republic of China

² Shenyang Medical College, No146 Huanghe North Street, Shenyang 110034, People's Republic of China

examinations in rat exposure to fluoride appeared thickening and disappearance of dendrites, swelling of mitochondria, dilation of the endoplasmic reticulum in neurons [8, 9], and impaired hippocampus synaptic interface structure [10]. These data indicate that excessive exposure to fluoride results in structural and functional damages of the CNS and is associated with CNS dysfunction.

The mechanism of brain dysfunction due to chronic fluorosis has been thought by oxidative stress-mediated damage of brain tissues. Fluoride can induce oxidative damage and apoptosis in neurons, which might be regulated by antiapoptotic genes and death receptor-mediated pathway [11–13]. Fluoride affects the brain by inhibiting some enzymes associated with energy production and transfer, membrane transport, and synaptic transmission [14]. Chronic or subchronic fluoride exposure may lead to reduction of acetylcholinesterase activity and nicotinic acetylcholine receptor level, as well as alteration in the neurotransmitter level [15, 16]. The developmental neurotoxicity of fluoride may be closely associated with low glucose utilization and neurodegenerative changes [17]. The hippocampus is the key region for learning and memory in the brain and has been postulated to be one of the neurotoxic target sites attacked by fluoride [18]. Beta amyloid plaques were formed in the brain of fluoride-treated rats [19], which was similar to that occurring in patients with Alzheimer's disease (AD). AD is characterized by an abnormal increase of variety of inflammatory cytokines and chemokines in the brain which is associated with an immunological response of activated microglial cells [20]. Fluoride treatment could lead to degeneration of glial cells, and glial cells were as targets of fluoride toxicity and involved in dysfunction of the brain induced by fluoride [21, 22]. In addition, glial activation and inflammatory response were seen and a close link between oxidative stress neuroinflammation and degeneration in aluminum-fluoride toxicity rats was observed. Microglial cells were activated during fluoride- and aluminum-induced neuronal damage [23].

Microglia serve as the resident immune cells of the CNS and comprise about 10–15 % of the total cell population of the brain. Under physiologic conditions in the intact, healthy CNS, microglial cells exhibit a ramified morphology with a small, round soma, and various branching processes. Microglia change their morphology and function in response to a given stimulus and present amoeboid form with characteristic macrophage functions [24]. Microglia are the first line of defense that respond rapidly to any type of brain injury [25]. But, chronic microglial activation appears to cause neuronal damage through producing potentially neurotoxic substances such as proinflammatory cytokines, reactive oxygen intermediates, proteinases, and complement proteins [26]. These cytokines can act on astrocytes to induce a secondary inflammatory or growth factor repair response [27]. Numerous studies suggest that chronic microglial activation is harmful for neuronal

survival. High interleukin-1 β (IL-1 β) concentrations in the hippocampus are associated with impaired memory [28]. For many neurodegenerative disorders, activated microglia are the hallmark of neuroinflammation [29].

In our previous studies *in vitro* [30], it was found that fluoride treatment enhanced ROS levels and the release of inflammatory cytokines by inducing the activities of BV-2 microglia. To demonstrate these findings, this study examined the microglia phenotype and pro-inflammatory cytokine expressions in the hippocampus and cortex of fluoride-treated rats *in vivo*. Here, we provide evidence that chronic microglia activation and release of proinflammatory cytokines is consistent in the hippocampus and cortex of fluoride-treated rats. Importantly, these data suggest that chronic activation of microglia in fluoride-treated rat brain could play a part in the dysfunction of CNS.

Material and Methods

Chemicals

Sodium fluoride (NaF) was procured from Sigma Chemical (St. Louis, MO, USA). Anti-Bax, anti-Bcl-2, anti-IL-1 β , anti-IL-6, and anti-tumor necrosis factor- α (TNF- α) antibodies were obtained from Sangon Biotech Co., Ltd. (Shanghai, China), and anti-OX-42 antibody was purchased from Cell Signaling Technology (Beverly, MA, USA). All other reagents used were of analytical grade, and deionized water was used throughout the study. Stock solutions of NaF (120 g/l) were prepared and stored in the dark at 4 °C. Diluted standard solutions for study were prepared fresh daily.

Animals and Treatment

Thirty male and 30 female healthy adult Wistar rats were obtained at 5 weeks of age from Experimental Animal Center of China Medical University (China). The animals were acclimated for a week before the start of the experiment and fed common basal pellet diet and water *ad libitum*. Rats were assigned randomly to three groups containing 20 rats per group by body weight stratification. NaF-treated rats received 60 and 120 parts per million (ppm, milligrams per liter) of fluoride ion (F⁻) in drinking water for 10 weeks. Control rats received deionized water (no added NaF) for 10 weeks. During the course of treatment, rats were observed daily for any clinical signs and daily water consumption, body weight gain, and feed consumption were recorded periodically. The actual intake of the fluoride was calculated from water consumption data. All of the rats were kept in ventilated cages at 23–27 °C, with 55–60 % humidity and 12/12 h light/dark cycles. After 10 weeks, exposure was stopped and rats were sacrificed under anesthesia of 10 % chloral hydrate, 0.3 ml/100 g body

weight via intraperitoneal injection. Blood samples were drawn via the abdominal aorta for the separation of serum from 10 rats of each group, the brains of 8 rats were resected and weighed, and the relative weight of brain (%) was calculated as grams per 100 g body weight. The whole hippocampus and cerebral cortex were dissected from the brain for Western blot analysis and F^- determine. The brains of other two rats were fixed in 2.5 % glutaraldehyde for pathological examination by transmission electron microscopy (TEM). Another 10 rats of each group were perfused through the heart with 100 ml of normal saline containing 0.02 % heparin, followed by 200–400 ml of 4 % paraformaldehyde in 0.1 M potassium phosphate buffer (pH=7.4). After perfusion, the brain was removed quickly and post-fixed in the same fixing solution at room temperature for overnight. The fixed brains were cut coronally and routinely embedded in paraffin for immunofluorescence analysis and terminal deoxynucleotidyl transferase-mediated dUTP nick-end labeling (TUNEL) text. All samples were stored at $-80\text{ }^\circ\text{C}$ until analysis. The experimental procedure used in this study met the guidelines of the Animal Care and Use Committee of the China Medical University.

Determination of Fluoride

The fluoride ion (F^-) level in serum (10 rats each group) was measured potentiometrically directly after dilution with equal volumes of total ionic strength adjustment buffer using a fluoride ion-specific electrode, and results were expressed as micrograms per milliliter. The concentration of F^- in the brain (8 rats each group) was determined according to the method of enzyme standard instrument-fluorine reagent colorimetric method [31]. Briefly, about 50 mg of brain tissue digested with lipase and protease was dissolved in an acid mixture (nitric acid and argent nitrate) in a closed compartment. The cover of the compartment was overlaid with saturation sodium hydroxide. After neutralization for 24 h, fluorine reagent was added into the mixture, and the values were calculated from a standard curve. The amount of fluoride was expressed in microgram of fluoride per gram of dry tissue.

Transmission Electron Microscopy Analysis

Brain tissues fixed with 2.5 % glutaraldehyde were post-fixed in 1 % osmium tetroxide, dehydrated through graded ethanol series, and embedded in Spurr's resin. Resin sections of 50 nm were cut on resin microtome, and ultrathin sections were stained with uranyl acetate and lead citrate then observed ultrastructural changes of brain cells and photographed using JEM-1200EX (Hitachi Ltd., Tokyo, Japan) transmission electron microscope (TEM).

TUNEL Assay

To determine apoptosis, brain sections were stained with the terminal deoxynucleotidyl transferase-mediated dUTP nick-end labeling (TUNEL) reagents, which measures the nuclear DNA fragmentation, an important indicator of apoptosis. The TUNEL assay was performed according to the manufacture guidance of One Step TUNEL Apoptosis Assay Kit (Beyotime, Jiangsu, China). Briefly, the brains embedded in paraffin were sectioned into 6- μm thick coronal sections. The tissue sections were deparaffinized in xylene for 10 min and hydrated through a graded ethanol series. Then, the tissue sections were treated with proteinase K solution and incubated in TUNEL reaction mixture for 1 h at $37\text{ }^\circ\text{C}$ in a humidified chamber. After washing with phosphate buffer solution (PBS), randomly chosen fields were examined under fluorescence microscopy (LEICA DMILLED, Germany). TUNEL-positive cells were deemed to be undergoing apoptosis and appeared red in the nucleus and with an irregular shape. The immunoreactive area was measured using a computer-assisted image analysis program (Image-pro plus 6.0). The area of highlighted immunoreactivity was calculated as average signal intensity of the selected field. The sections were microscopically obtained at a magnification of $\times 200$ (objective $\times 20$ and ocular $\times 10$).

Western Blot Analysis

The hippocampus and cerebral cortex samples were lysed in ice-cold lysis buffer by supersound and then centrifuged at 12,000g for 25 min at $4\text{ }^\circ\text{C}$. Protein quantification of the supernatant was performed using the protein assay kit. Lysates with 30 μg protein each were subjected to electrophoresis on 10 % SDS-polyacrylamide gel electrophoresis and transferred to a polyvinylidene difluoride (PVDF) membrane (Millipore, Bedford, USA) at 100 V for 1 h. After the membranes were blocked in 5 % fat-free dry milk in Tween 20 Tris-buffered saline (TBST) for 1 h, the membranes were incubated with primary antibodies at a dilution of 1:500 anti-Bcl-2 and anti-Bax and 1:3000 polyclonal antibodies to β -actin, overnight at $4\text{ }^\circ\text{C}$. After washed with TBST, the membranes were incubated in horseradish peroxidase-conjugated secondary antibody (1:5000) for 1 h and washed with TBST three times. Protein bands were detected by enhanced chemiluminescence reagent and then densitometric analysis was performed with an LI-COR Odyssey Infrared Imaging system.

Double Immunofluorescence

The brains embedded in paraffin were sectioned into 6- μm thick coronal sections. The brains were sectioned in a serial manner when intact structure of the hippocampus was observed in the slices. Every fifth/sixth slices were collected

per animal on gelatin-coated microscope slides. Three sections were selected randomly from each rat brain. Microglial cells were identified by specific labeling with CD11b (OX-42), a constitutive marker of microglia and is frequently present on activated microglia. After being deparaffinized in xylene for 10 min followed by 100 % ethanol, the slices were washed three times in phosphate buffered saline (PBS). After preincubation in 10 % normal goat serum at room temperature for 30 min, the sections were incubated with mouse anti-OX-42 monoclonal antibody (1:100 dilution) along with rabbit anti-IL-6 or with rabbit anti-TNF- α or with rabbit anti-IL-1 β polyclonal antibody (1:50 dilution) overnight at 4 °C. Tissue sections were then washed three times in PBS. The sections were incubated with a second antibody conjugated to the fluorescent markers FITC and TRITC (1:50; Boster Biotech Co., Ltd. Wuhan, China) at room temperature for 2 h. Then, the slices were washed three times in PBS. At last, the slices were mounted with glycerin gelatin for histological examination. Photo images were captured from the hippocampus and cortex by fluorescence microscope (LEICA DMILLED, Germany). The immunoreactive area was measured using a computer-assisted image analysis program (Image-Pro Plus 6.0). The area of highlighted immunoreactivity was calculated as average signal intensity of the selected field. The sections were microscopically obtained at a magnification of $\times 200$ (objective $\times 20$ and ocular $\times 10$).

Statistical Analysis

SPSS 13.0 (SPSS Inc., Chicago, IL, USA) was used for the analysis. One-way analysis of variance (ANOVA) was used to evaluate the difference among groups. Experimental results were expressed as the mean \pm SD, and a $p < 0.05$ was considered significant in all tests.

Results

General Observations

No significant toxic symptom was observed except for dental fluorosis in the 60 and 120 ppm fluoride-treated rats as expected. Water consumption of the fluoride-treated rat groups decreased slightly compared with the control group (data not shown). Analysis of body weight throughout the experiment showed that there was no difference between 60 ppm fluoride-treated group and control rats. But body weight of 120 ppm fluoride-treated rats decreased from the seventh week of exposure to NaF, see Fig. 1. The fluoride intake was calculated according to water consumption amount and increased proportionally to water fluoride concentration.

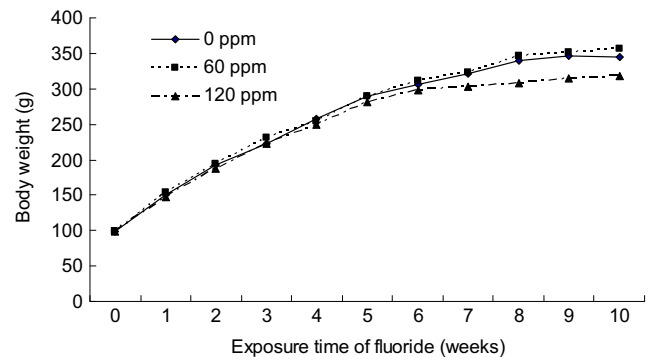


Fig. 1 Effects of fluoride on the body weight of rats. Data were displayed as the means of 20 replicates

The Concentrations of Fluoride in the Serum and Brain Tissues

Dose-dependent increases of concentrations of fluoride in the serum ($r = 0.813$, $p < 0.01$) and brain tissues ($r = 0.787$, $p < 0.01$) were observed in rats exposed to NaF. Table 1 showed that fluoride concentrations in the serum and brain tissues of 60 and 120 ppm fluoride-treated rats were significantly higher than that of control rats ($p < 0.01$).

Ultrastructure Observation of the Brain

Transmission electron microscope (TEM) analysis of the ultrastructure of the brain in rats was showed in Fig. 2. In the control group, the brain exhibited normal integral structures, and the brain cells showed one or more oval nuclei with visible clear nucleoli and double nuclear membranes, abundant mitochondria, endoplasmic reticulum, and ribosomes in the cytoplasm of the brain cells (Fig. 2a). In 60 ppm fluoride-treated rats, brain cells appeared cytomorphic, with intranuclear heterochromatin margination condensation, mitochondrial outer membrane: part vague, rough endoplasmic reticulum: gently expanding, cellular membrane: part swollen. In the rats treated with 120 ppm fluoride, brain cells appeared obviously intranuclear heterochromatin margination aggregated, cellular membrane dissolved, with shrinkage of nuclear and cell volume, organelle dissolved, and apoptosis presented.

Apoptosis of Neurons in the Rat Brain

The apoptotic cells appeared red under immunofluorescence. The density of immunofluorescence in the cortex and hippocampus was significantly different between fluoride-treated rats and the control rats. Figure 3 showed higher TUNEL-positive immunofluorescence in the cortex and hippocampus in 60 and 120 ppm fluoride-treated rats compared with the control groups. TUNEL-positive staining increased with increasing fluoride concentrations. The intensities of

Table 1 The concentrations of F⁻ in the serum and brain tissues of NaF-treated rats

| Groups | Serum (μg/ml) | brain tissues (μg/g) | |
|---------|---------------|----------------------|------------------|
| | <i>n</i> | $\bar{x} \pm SD$ | $\bar{x} \pm SD$ |
| Control | 10 | 0.077±0.057 | 0.266±0.136 |
| 60 ppm | 10 | 0.148±0.044* | 0.655±0.202** |
| 120 ppm | 10 | 0.394±0.135**## | 0.997±0.359**## |

* $p < 0.05$ compared with the control group; ** $p < 0.01$ compared with the control group; # $p < 0.05$ compared with 60 ppm fluoride-treated group; ## $p < 0.01$ compared with 60 ppm fluoride-treated group

fluorescence in the cortex and hippocampus in fluoride-treated rats increased in a dose-dependent manner ($r=0.635$, $p=0.000$ and $r=0.928$, $p=0.000$, respectively).

Bax and Bcl-2 Expressions in the Brain of Rats

Expressions of Bax and Bcl-2 in the brain were measured by Western blot analysis, as shown in Fig. 4. The protein expressions of Bax in the hippocampus dramatically increased in 120 ppm fluoride-treated rats compared with the control group rats, and there was a dose-dependent correlation between expression of Bax and fluoride concentration ($r=0.550$, $p=0.018$). Bcl-2 expression level in the cortex decreased in 120 ppm fluoride-treated rats when compared to the control group rats ($p < 0.05$). A negative correlation was found between Bcl-2 expression and fluoride concentration in the cortex ($r=-0.504$, $p=0.033$). In addition, expressions of Bax in the cortex increased and Bcl-2 expressions in hippocampus decreased, but there were no significant differences between fluoride-treated rats and control rats. We calculated the index of Bcl-2/Bax to evaluate proliferation and apoptosis of brain cells. It was shown that indexes of Bcl-2/Bax in the hippocampus decreased with fluoride concentration ($r=-0.681$, $p=0.002$), and indexes of Bcl-2/Bax in the hippocampus of 60 and 120 ppm fluoride-treated groups were significantly lower than those of the control group, which meant fluoride promoting apoptosis in rat brain.

Effects of Fluoride on the Inflammatory Factor Expressions in the Hippocampus and Cortex Region in OX-42-Labeled Microglial Cells

Microglial activation was assessed in rats by analyzing brain tissue sections immunostained with OX-42, a marker of activated microglia in rats. The activation of microglial cells in the hippocampus and cortex of fluoride-treated rats is confirmed in this study using anti-OX-42 antibody. OX-42 immunoreactivity in the hippocampus and cortex of 60 and 120 ppm fluoride-treated rats dramatically increased compared with that of the control rats ($p < 0.05$), shown in Fig. 5. In the hippocampus of fluoride-treated rats, OX-42-positive microglial cells were more abundant than in the cortex. The level of IL-1 β protein expression in OX-42-labeled microglial cells was significantly increased in the cortex of rats exposed to 60 ppm fluoride and the hippocampus of rats exposed to 120 ppm fluoride (Fig. 6), but no statistical changes were observed in the cortex of rats exposed to 120 ppm fluoride. The expressions of IL-6 in OX-42-labeled microglial cells were greatly increased in the cortex and hippocampus of rats exposed to 60 and 120 ppm fluoride when compared to control rats, and there was a positive dose-dependent correlation in the cortex and hippocampus ($r=0.916$, $p < 0.01$ and $r=0.833$, $p < 0.01$, respectively), seen Fig. 7. The TNF- α immunoreactivity in the hippocampus was significantly higher in the 120 ppm fluoride-treated group than in the control group ($p < 0.05$). We observed no significant differences for TNF- α immunoreactivity in the cortex among groups, see Fig. 8.

Fig. 2 The ultrastructure of the brain cells in rats. **a** The brain of control rat; **b** the brain of rat exposed to 60 mg/l fluoride; **c** the brain of rat exposed to 120 mg/l fluoride. *Nu* nucleolus, *NM* nuclear membrane, *CC* chromatin condensation, *MS* mitochondria swelling, *MD* membrane dissolving. Magnification, $\times 6000$

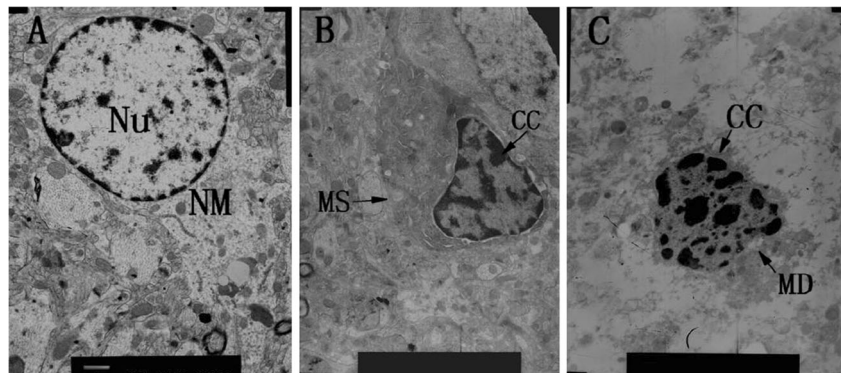


Fig. 3 TUNEL text showed the positive apoptotic neurons in the cortex and hippocampus of fluoride-treated rats. The red fluorescence represented the apoptotic cells. The pictures were representative images. Bars were presented as mean±SD. ** $p < 0.01$ compared to control group, ### $p < 0.01$ compared to 60 ppm group. Magnification, ×200

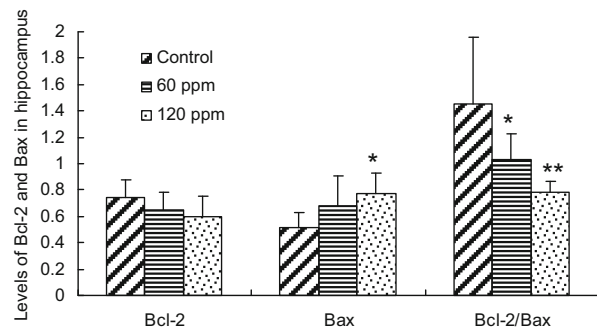
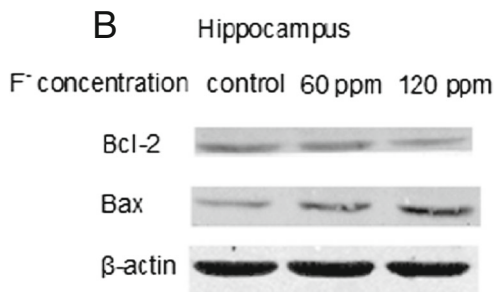
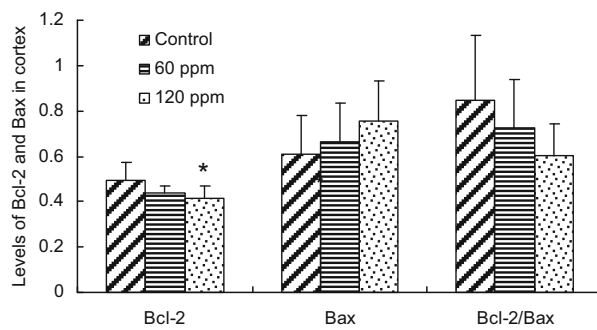
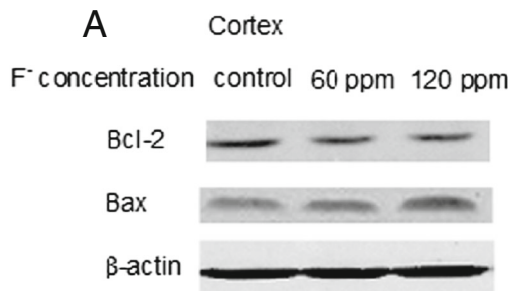
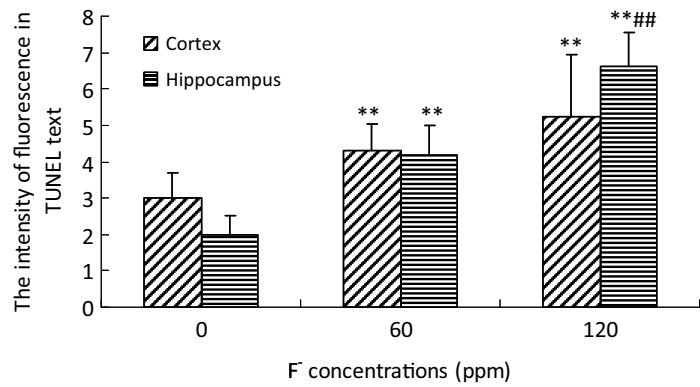
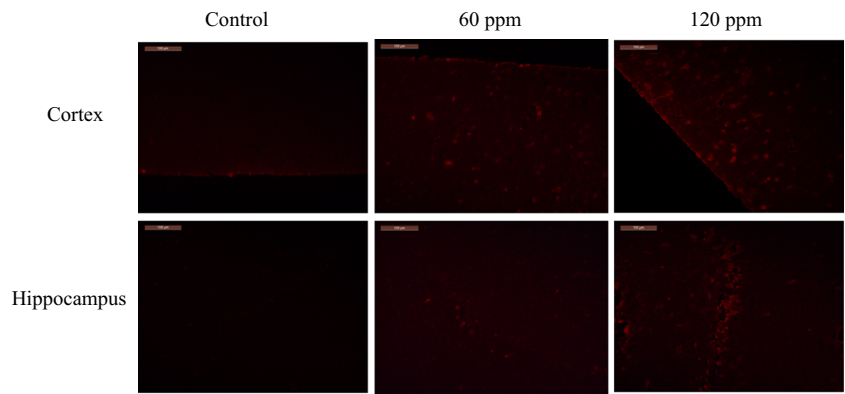
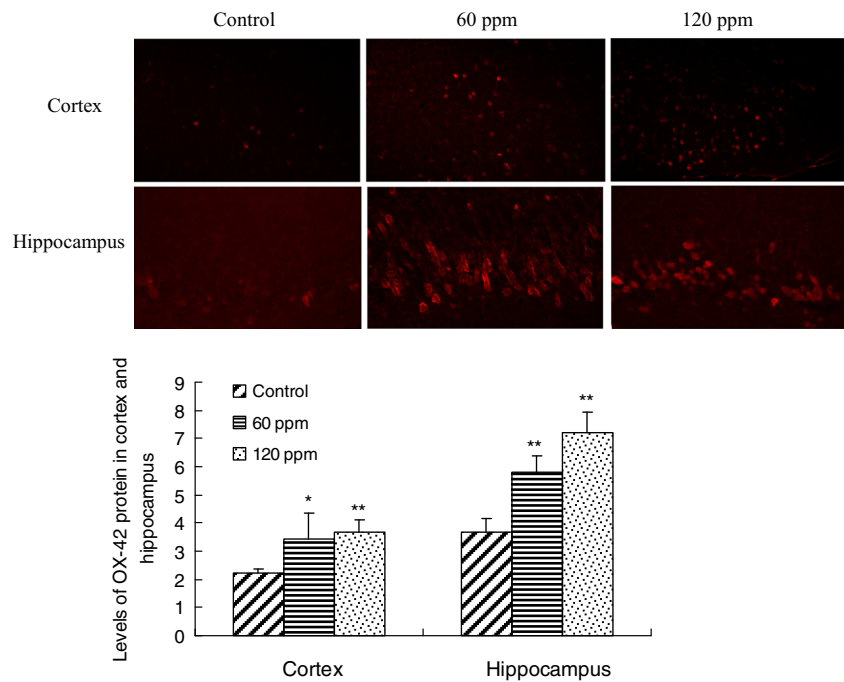


Fig. 4 The expressions of Bcl-2 and Bax in the cortex and hippocampus of rats. **a** Cortex; **b** hippocampus. The representative Western blot was showed in the left panel. The right panel was a graphical representation of

the relative densitometry of these bands. Loading was normalized to β -actin. Bars were presented as mean±SD. * $p < 0.05$ compared to control group, ** $p < 0.01$ compared to control group

Fig. 5 OX-42 immunoreactivity of microglia in the cortex and hippocampus. The representative microglia immunolabeled using OX-42 (red) was showed in the upper pictures. The panel below was a graphical representation of the relative intensity of the selected field. Bars were presented as mean±SD. * $p<0.05$ compared to control group, ** $p<0.01$ compared to control group. Magnification, $\times 200$



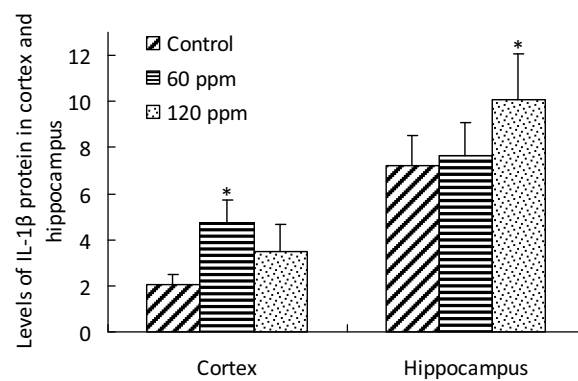
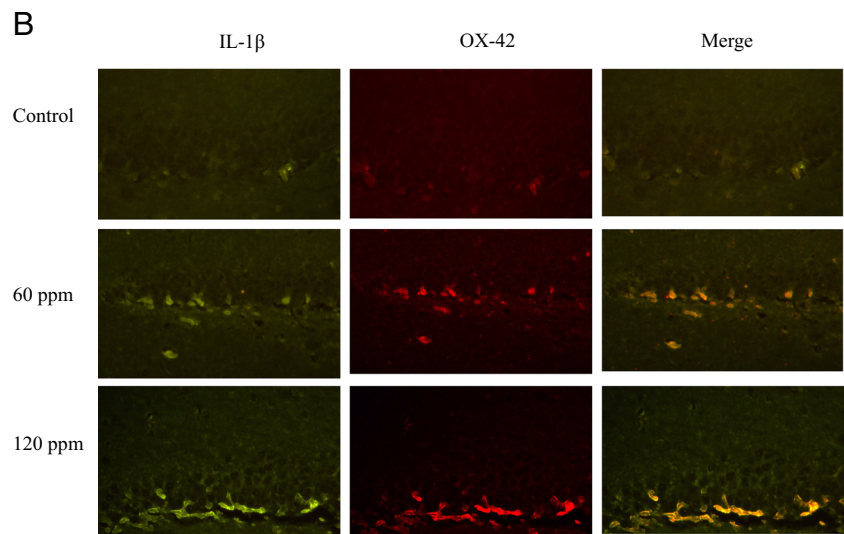
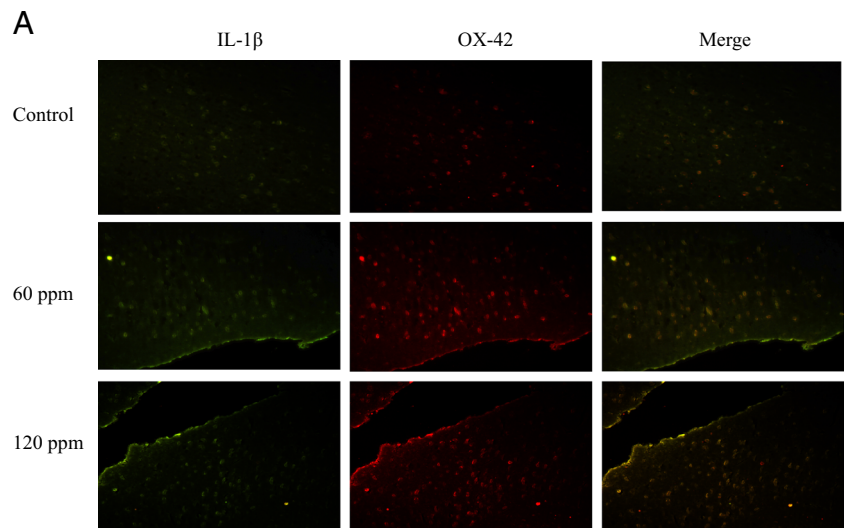
Discussion

A number of studies reported neuropathological lesions in chronic and high dose of fluoride treated brain, such as chromatolysis of Purkinje neurons, damage to the neurons and neuroglial cells, and neurodegenerative changes in rat brain [17]. However, the molecular mechanism underlying the pathogenesis of CNS damage induced by chronic fluorosis remains elusive. Many studies linked fluoride-induced brain changes through oxidative stress [11, 32]. It is well known that oxygen-derived free radicals are a major source for DNA damage, which can cause strand breaks and base alteration in the DNA and elicits apoptosis [33]. Apoptosis is a genetically controlled mechanism of cell death involved in regulation of tissue homeostasis. Bcl-2 blocks apoptosis by stabilizing the mitochondrial membrane, whereas Bax induces apoptosis by increasing the mitochondrial membrane permeability [34]. TUNEL text can detect DNA fragments in situ by terminal deoxynucleotidyl transferase-mediated dUTP nick end labeling and provide accurate detection of apoptotic cells. In this study, apoptosis in the hippocampus and cortex of fluoride-treated rats were found by TUNEL text and apoptotic rate of excessive fluoride exposed hippocampus and cortex was showed in a dose-dependent manner, similar to the report of Liu [35]. Moreover, we also found that Bax protein expressions in the hippocampus dramatically increased and Bcl-2 expressions in the cortex decreased in 120 ppm fluoride-treated rats compared with the control group rats, and indexes of Bcl-2/Bax in the hippocampus and cortex decreased with fluoride concentration increase. The proteins involved in proliferation and death appeared promoting apoptosis in fluoride-

exposed rat brain. We also observed here ongoing intranuclear heterochromatin margination aggregation, cellular membrane dissolution, shrinkage of nuclear and cell volume, organelle dissolution, and apoptosis presented in the hippocampus and cortex of high-fluoride-exposed rats by electron microscopy. Generally, these changes were thought related with oxidative stress and pro-inflammatory factors, which might make a contribution to the related brain injury.

Recently, it is reported that increases of microglia activation and inflammatory response were seen in aluminum, fluoride, and a combination of aluminum–fluoride-treated rat brain [23]. Microglia are the resident immune cell population of the CNS and are highly sensitive to physiological and pathological changes. Microglia are implicated in the regulation of neural homeostasis and the response to injury and repair and express low levels of cytokines and chemokines in the healthy brain [36, 37]. Microglia are activated as given stimulus through changing their morphology and function. A well-known marker of activated microglia is CD11b (OX-42) expression. Microglial activation in this study was evidenced by the increased amount of OX-42-positive cells in fluoride-treated rat brain. Activated microglia cells produce several inflammatory cytokines such as TNF- α , IL-1 β , and IL-6, which are critical in regulating the physiological immune responses in the CNS [38, 39]. However, under pathological conditions, activated microglia can secrete excessive pro-inflammatory cytokines, which were involved in tissue damage and neuronal dysfunction [40]. Microglial activation is considered to be a hallmark of neuroinflammation in the brain. In addition, chronic activation of microglia excessively prolongs the inflammatory response and causes neuronal damage, which triggers the development

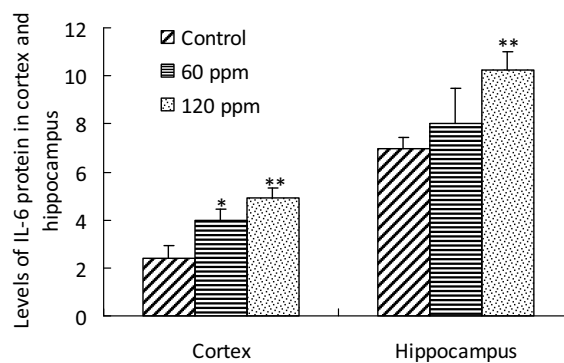
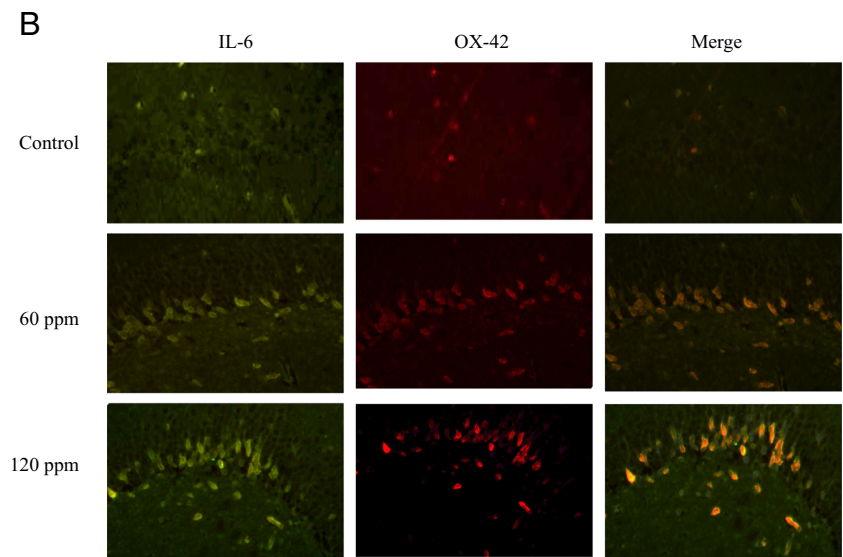
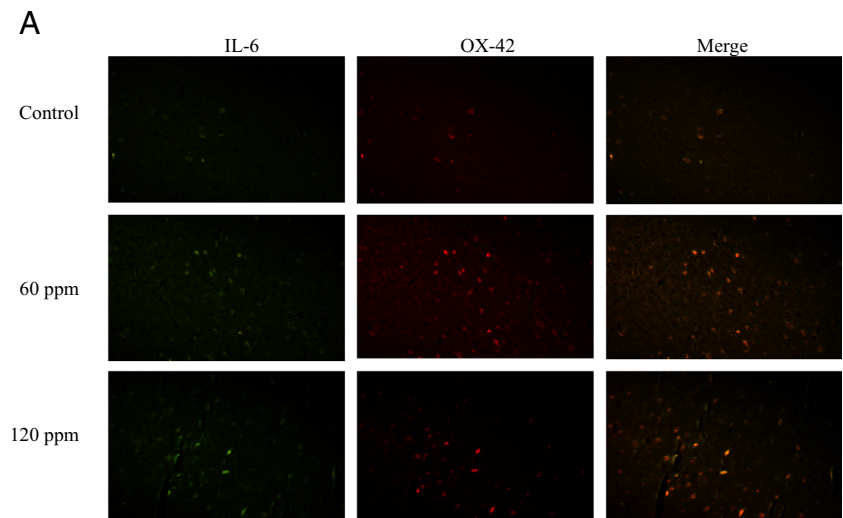
Fig. 6 IL-1 β expression in microglia of fluoride-treated rats. IL-1 β immunofluorescence analysis showed green expression and microglia immunolabeled using OX-42 (red). **a** Cortex; **b** hippocampus. The panel below was a graphical representation of the relative intensity of the selected field. Bars were presented as mean \pm SD. * p <0.05 compared to control group. Magnification, \times 200



of neurodegenerative diseases [39]. In this model, there is persistent microglial activation in rat brain of subchronic exposure to fluoride as compared to the control rats. We observed that pro-inflammatory cytokines IL-1 β , IL-6, and TNF- α immunostaining co-localized with the microglia marker OX-42. The

expressions of IL-1 β , IL-6, and TNF- α in microglia were increased in a dose-dependent manner, in line with a previous study in vitro [30]. Our results suggested that fluoride may affect immune responses within the CNS and can potentiate inflammatory responses of microglia to fluoride stimulation.

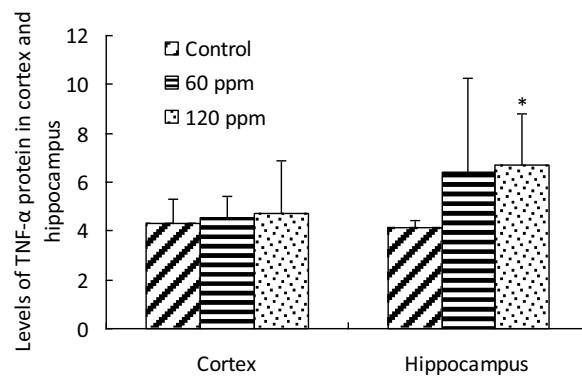
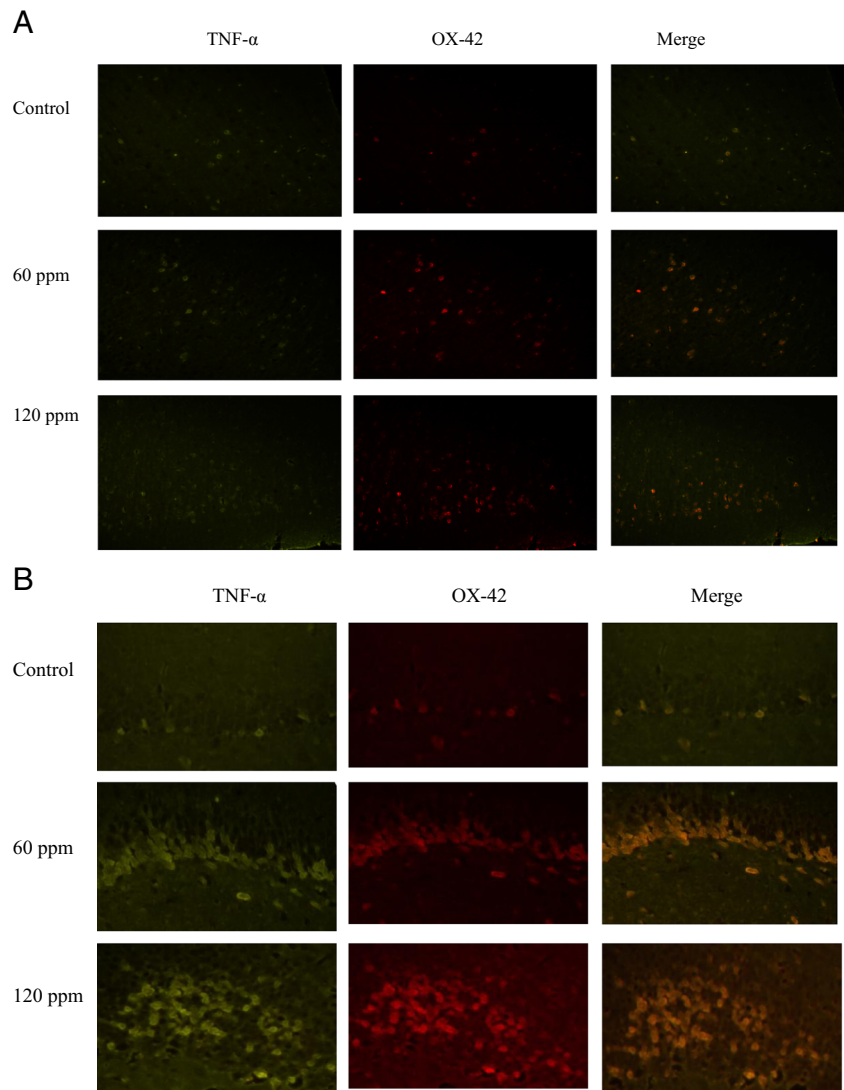
Fig. 7 IL-6 expression in microglia of fluoride-treated rats. IL-6 immunofluorescence analysis showed green expression and microglia immunolabeled using OX-42 (red). **a** Cortex; **b** hippocampus. The panel below was a graphical representation of the relative intensity of the selected field. Bars were presented as mean±SD. * $p < 0.05$ compared to control group, ** $p < 0.01$ compared to control group. Magnification $\times 200$



In the present study, the number of microglia was markedly increased in the hippocampus compared with the cortex. The hippocampus has a higher density of microglia than other brain regions [41]. Learning and memory has been associated with hippocampal activity [42]. It has been reported that

impaired spatial memory performance might be due to fluoride accumulation in brain areas especially in the hippocampus [43]. The IL-1 β is induced within the hippocampus in response to normal learning, and physiological level of IL-1 β is critical for maintaining long-term potentiation (LTP)

Fig. 8 TNF- α expression in microglia of fluoride-treated rats. TNF- α immunofluorescence analysis showed green expression and microglia immunolabeled using OX-42 (red). **a** Cortex; **(b)** hippocampus. The *panel below* was a graphical representation of the relative intensity of the selected field. Bars were presented as mean \pm SD. * p <0.05 compared to control group. Magnification, \times 200



[44]. Microglia are the primary source of IL-1 β within the hippocampus during normal learning [45]. However, a high level of IL-1 β can profoundly impair memory and is associated with neurodegenerative disorders [46, 47]. The developmental neurotoxicity of fluoride may be closely associated with neurodegenerative changes [17]. The suppression of the

inflammatory activation of microglia might play a part in ameliorated cognitive deficits [48]. Microglia activation is a key causative factor in neurodegeneration [49]. NaF-treated rat displayed neurodegenerative changes [17]. Neurodegeneration initiated by microglia can be driven through TNF- α signaling [50]. TNF- α can activate receptor-mediated

proapoptotic pathways within the neuron [51]. TNF- α is predominantly produced by microglia after many forms of injury [52]. Increased levels of TNF- α have been associated with the pathological effects of a variety of infectious, neurological, neurodegenerative, and neurotoxic conditions [53]. Our results showed that TNF- α expression significantly increased in fluoride-treated rat hippocampus.

Taken together, these results indicate that fluoride induced neuron apoptosis and expressions of inflammatory factors by activating microglia in rat brain. To our knowledge, this is the first time that changes of pro-inflammatory cytokine expressions in activated microglia were described in subchronic exposure to fluoride rats.

Acknowledgments This work was supported by the Research Fund for the Doctoral Program of Higher Education of China (No. 20112104110021).

Conflict of Interest The authors declare that they have no competing interests.

References

- Wang S, Wang Z, Cheng X, Li J, Sang Z, Zhang X, Han L, Qiao X et al (2007) Arsenic and fluoride exposure in drinking water: children's IQ and growth in Shanyin County, Shanxi province, China. *Environ Health Perspect* 115(4):643–647
- Trivedi MH, Verma RJ, Chinoy NJ, Patel RS, Sathawara NG (2007) Effect of high fluoride water on intelligence of school children in India. *Fluoride* 40:178–183
- Xiang Q, Liang Y, Chen L, Wang C, Chen B, Chen X, Zhou M (2003) Effect of fluoride in drinking water on children's intelligence. *Fluoride* 36:84–94
- Tang Q, Du J, Ma H, Jian S, Zhou X (2008) Fluoride and children's intelligence, a meta-analysis. *Biol Trace Elem Res* 126(1–3):115–120
- Spittle B (1994) Psychopharmacology of fluoride: a review. *Int Clin Psychopharmacol* 9(2):79–82
- Chioca LR, Raupp IM, Da Cunha C, Losso EM, Andreatini R (2008) Subchronic fluoride intake induces impairment in habituation and active avoidance tasks in rats. *Eur J Pharmacol* 579(1–3):196–201
- Liu F, Ma J, Zhang H, Liu P, Liu YP, Xing B, Dang YH (2014) Fluoride exposure during development affects both cognition and emotion in mice. *Physiol Behav* 124:1–7
- Guan Z, Wang Y, Xiao K, Dai D, Chen Y, Liu J, Sindelar P, Dallner G (1998) Influence of chronic fluorosis on membrane lipids in rat brain. *Neurotoxicol Teratol* 20(5):537–542
- Shashi A (2003) Histopathological investigation of fluoride-induced neurotoxicity in rabbits. *Fluoride* 36:95–105
- Zhang Z, Xu X, Shen X (2008) Effect of fluoride exposure on synaptic structure of brain areas related to learning-memory in mice. *Fluoride* 41:139–143
- Zhang M, Wang A, He W, He P, Xu B, Xia T, Chen X, Yang K (2007) Effects of fluoride on the expression of NCAM, oxidative stress, and apoptosis in primary cultured hippocampal neurons. *Toxicology* 236(3):208–216
- Adebayo OL, Shallie PD, Salau BA, Ajani EO, Adenuga GA (2013) Comparative study on the influence of fluoride on lipid peroxidation and antioxidants levels in the different brain regions of well-fed and protein undernourished rats. *J Trace Elem Med Biol* 27(4):370–374
- Lee JH, Jung JY, Jeong YJ, Park JH, Yang KH, Choi NK, Kim SH, Kim WJ (2008) Involvement of both mitochondrial- and death receptor-dependent apoptotic pathways regulated by Bcl-2 family in sodium fluoride-induced apoptosis of the human gingival fibroblasts. *Toxicology* 243(3):340–347
- Pal S, Sarkar C (2014) Protective effect of resveratrol on fluoride induced alteration in protein and nucleic acid metabolism, DNA damage and biogenic amines in rat brain. *Environ Toxicol Pharmacol* 38(2):684–699
- Long Y, Wang Y, Chen J, Jiang S, Nordberg A, Guan Z (2002) Chronic fluoride toxicity decreases the number of nicotinic acetylcholine receptors in rat brain. *Neurotoxicol Teratol* 24(6):751–757
- Pereira M, Dombrowski P, Losso E, Chioca L, DaCunhaC AR (2011) Memory impairment induced by sodium fluoride is associated with changes in brain monoamine levels. *Neurotoxicol Res* 19(1):55–62
- Jiang C, Zhang S, Liu H, Guan Z, Zeng Q, Zhang C, Lei R, Xia T et al (2014) Low glucose utilization and neurodegenerative changes caused by sodium fluoride exposure in rat's developmental brain. *Neuromol Med* 16(1):94–105
- Bhatnagar M, Rao P, Sushma J, Bhatnagar R (2002) Neurotoxicity of fluoride: neurodegeneration in hippocampus of female mice. *Indian J Exp Biol* 40(5):546–554
- Vamer JA, Jensen KF, Horvath W, Isaacson RL (1998) Chronic administration of aluminium fluoride and sodium fluoride in rats in drinking water, alterations in neuronal and cerebrovascular integrity. *Brain Res* 784(1–2):284–298
- Morales I, Guzman-Martinez L, Cerda-Troncoso C, Farias GA, Maccioni RB (2014) Neuroinflammation in the pathogenesis of Alzheimer's disease. A rational framework for the search of novel therapeutic approaches. *Front Cell Neurosci* 8:112
- Trabelsi M, Guermazi F, Zeghal N (2001) Effect of fluoride on thyroid function and cerebellar development in mice. *Fluoride* 34:165–173
- Flores-Méndez M, Ramírez D, Alamillo N, Hernández-Kelly LC, Del Razo LM, Ortega A (2014) Fluoride exposure regulates the elongation phase of protein synthesis in cultured Bergmann glia cells. *Toxicol Lett* 229(1):126–133
- Akinrinade ID, Memudu AE, Ogundele OM, Ajetunmobi OI (2015) Interplay of glia activation and oxidative stress formation in fluoride and aluminium exposure. *Pathophysiology* 22(1):39–48
- Beynon SB, Walker FR (2012) Microglial activation in the injured and healthy brain: what are we really talking about? Practical and theoretical issues associated with the measurement of changes in microglial morphology. *Neuroscience* 225:162–171
- Hanisch UK, Kettenmann H (2007) Microglia: active sensor and versatile effector cells in the normal and pathologic brain. *Nat Neurosci* 10(11):1387–1394
- Perry VH (2004) The influence of systemic inflammation on inflammation in the brain: implications for chronic neurodegenerative disease. *Brain Behav Immun* 18(5):407–413
- Saijo K, Winner B, Carson CT, Collier JG, Boyer L, Rosenfeld MG, Gage FH, Glass CK (2009) A Nurr1/CoREST pathway in microglia and astrocytes protects dopaminergic neurons from inflammation-induced death. *Cell* 137(1):47–59
- Barrientos RM, Sprunger DB, Campeau S, Watkins LR, Rudy JW, Maier SF (2004) BDNF mRNA expression in rat hippocampus following contextual learning is blocked by intrahippocampal IL-1beta administration. *J Neuroimmunol* 155(1–2):119–126
- Block ML, Hong JS (2005) Microglia and inflammation-mediated neurodegeneration: multiple triggers with a common mechanism. *Prog Neurobiol* 76(2):77–98
- Yan L, Liu S, Wang C, Wang F, Song Y, Yan N, Xi S, Liu Z et al (2013) JNK and NADPH oxidase involved in fluoride-induced

- oxidative stress in BV-2 microglia cells. *Mediat Inflamm* 2013: 895975
31. Zhang ZY, Han B, Qian C (2011) Rapid detection method for trace fluoride with microplate reader. *Chin J Public Health* 27:255–256 (in Chinese)
 32. Sarkar C, Pal S, Das N, Dinda B (2014) Ameliorative effects of oleanolic acid on fluoride induced metabolic and oxidative dysfunctions in rat brain: experimental and biochemical studies. *Food Chem Toxicol* 66:224–236
 33. Roos WP, Kaina B (2006) DNA damage-induced cell death by apoptosis. *Trends Mol Med* 12(9):440–450
 34. Negrín G, Rubio S, Marrero MT, Quintana J, Eiroa JL, Triana J, Estévez F (2015) The eudesmanolide tanapsin from *Tanacetum oshanahanii* and its acetate induce cell death in human tumor cells through a mechanism dependent on reactive oxygen species. *Phytomedicine* 22(3):385–393
 35. Liu YJ, Guan ZZ, Gao Q, Pei JJ (2011) Increased level of apoptosis in rat brains and SH-SY5Y cells exposed to excessive fluoride—a mechanism connected with activating JNK phosphorylation. *Toxicol Lett* 204(2–3):183–189
 36. Harry GJ (2013) Microglia during development and aging. *Pharmacol Ther* 139(3):313–326
 37. Parakalan R, Jiang B, Nimmi B, Janani M, Jayapal M, Lu J, Tay SS, Ling EA et al (2012) Transcriptome analysis of amoeboid and ramified microglia isolated from the corpus callosum of rat brain. *BMC Neurosci* 13:64
 38. Sadasivan S, Pond BB, Pani AK, Qu C, Jiao Y, Smeyne RJ (2012) Methylphenidate exposure induces dopamine neuron loss and activation of microglia in the basal ganglia of mice. *PLoS ONE* 7:e33693
 39. Smith JA, Das A, Ray SK, Banik NL (2012) Role of pro-inflammatory cytokines released from microglia in neurodegenerative diseases. *Brain Res Bull* 87(1):10–20
 40. Zhang B, West EJ, Van KC, Gurkoff GG, Zhou J, Zhang XM, Kozikowski AP, Lyeth BG (2008) HDAC inhibitor increases histone H3 acetylation and reduces microglia inflammatory response following traumatic brain injury in rats. *Brain Res* 1226:181–191
 41. Lawson LJ, Perry VH, Dri P, Gordon S (1990) Heterogeneity in the distribution and morphology of microglia in the normal adult mouse brain. *Neuroscience* 39(1):151–170
 42. Leussis MP, Bolivar VJ (2006) Habituation in rodents: a review of behaviour, neurobiology and genetics. *Neurosci Biobehav Rev* 30(7):1045–1064
 43. Basha PM, Sujitha NS (2012) Combined impact of exercise and temperature in learning and memory performance of fluoride toxicated rats. *Biol Trace Elem Res* 150(1–3):306–313
 44. Ross FM, Allan SM, Rothwell NJ, Verkhratsky A (2003) A dual role for interleukin-1 in LTP in mouse hippocampal slices. *J Neuroimmunol* 144(1–2):61–67
 45. Williamson LL, Sholar PW, Mistry RS, Smith SH, Bilbo SD (2011) Microglia and memory: modulation by early-life infection. *J Neurosci* 31(43):15511–15521
 46. Barrientos RM, Frank MG, Hein AM, Higgins EA, Watkins LR, Rudy JW, Maier SF (2009) Time course of hippocampal IL-1 beta and memory consolidation impairments in aging rats following peripheral infection. *Brain Behav Immun* 23(1):46–54
 47. Streit WJ (2010) Microglial activation and neuroinflammation in Alzheimer's disease: a critical examination of recent history. *Front Aging Neurosci* 2:22
 48. Furuya M, Miyaoka T, Tsumori T, Liaury K, Hashioka S, Wake R, Tsuchie K, Fukushima M et al (2013) Yokukansan promotes hippocampal neurogenesis associated with the suppression of activated microglia in Gunn rat. *J Neuroinflammation* 10:145
 49. Brown GC, Neher JJ (2010) Inflammatory neurodegeneration and mechanisms of microglial killing of neurons. *Mol Neurobiol* 41(2–3):242–247
 50. Iliev AI, Stringaris AK, Nau R, Neumann H (2004) Neuronal injury mediated via stimulation of microglial toll-like receptor-9 (TLR9). *FASEB J* 18(2):412–414
 51. Park KM, Bowers WJ (2010) Tumor necrosis factor-alpha mediated signaling in neuronal homeostasis and dysfunction. *Cell Signal* 22(7):977–983
 52. Kraft AD, McPherson CA, Harry GJ (2009) Heterogeneity of microglia and TNF signaling as determinants for neuronal death or survival. *Neurotoxicology* 30(5):785–793
 53. McCoy MK, Tansey MG (2008) TNF signaling inhibition in the CNS: implications for normal brain function and neurodegenerative disease. *J Neuroinflammation* 5:45